

CONVEXIFICATION FOR THE INVERSION OF A TIME DEPENDENT WAVE FRONT IN A HETEROGENEOUS MEDIUM*

MICHAEL V. KLIBANOV[†], JINGZHI LI[‡], AND WENLONG ZHANG[§]

Abstract. An inverse scattering problem for the 3D acoustic equation in time domain is considered. The unknown spatially distributed speed of sound is the subject of the solution of this problem. A single location of the point source is used. Using a Carleman Weight Function, a globally strictly convex cost functional is constructed. A new Carleman estimate is proven. Global convergence of the gradient projection method is proven. Numerical experiments are conducted.

Key words. Coefficient Inverse Problem, convexification, Carleman estimate, global strict convexity, numerical examples

AMS subject classifications. 35R30

1. Introduction. We develop analytically and test numerically a globally convergent numerical method for a Coefficient Inverse Problem (CIP) for the 3D acoustic equation in the time domain. The spatially distributed speed of sound is the subject of the solution of this CIP. Only a single location of the point source is used here. For reasons explained below, we call this method “convexification”. In the publication [18] of the first author a globally strictly convex cost functional was constructed for the same CIP for the first time. This paper is a deep revision of [18]. We significantly update the theory of [18]. Our goal is to make the theory of [18] computationally feasible. New results of this paper are (also, see Remark 4.1 in section 4):

1. We prove a new Carleman estimate for the Laplace’s operator (Theorem 4.1). This one is well suitable for computations. On the other hand, the Carleman estimate of [18] uses two large parameters and, therefore, changes too rapidly, which makes it inconvenient for computations.
2. Using the Carleman estimate of Theorem 4.1, we “convexify” our CIP, i.e. we construct a new weighted Tikhonov-like functional, which is strictly convex on a set $B(m, R)$ in a certain Hilbert space of an arbitrary “size” $R > 0$, where the number $m \in (0, R)$ is independent on R . Since the number $R > 0$ is an arbitrary one, then this is the *global strict convexity*. The key element of the above functional is the presence of the Carleman Weight Function (CWF) in it. Unlike [18], our functional contains a regularization parameter $\beta \in (0, 1)$. It is the presence of this parameter which allows us to work without an inconvenient assumption of [18] (the last paragraph of page 1379 of [18]) which is about working on a certain compact set. Unlike the latter, we consider here a more convenient case of the bounded set $B(m, R)$. We

*Submitted to the editors DATE.

Funding: The work of Klibanov was supported by US Army Research Laboratory and US Army Research Office grant W911NF-19-1-0044. The work of Li and Zhang was partially supported by the NSF of China under the grant No. 11571161 and 11731006, the Shenzhen Sci-Tech Fund No. JCYJ20160530184212170 and JCYJ20170818153840322.

[†]Department of Mathematics and Statistics, University of North Carolina at Charlotte, Charlotte, NC 28223, USA (mklibanv@uncc.edu)

[‡]Corresponding author. Department of Mathematics, Southern University of Science and Technology (SUSTech), 1088 Xueyuan Boulevard, University Town of Shenzhen, Xili, Nanshan, Shenzhen, Guangdong Province, P.R.China (li.jz@sustc.edu.cn)

[§]Department of Mathematics, Southern University of Science and Technology (SUSTech), 1088 Xueyuan Boulevard, University Town of Shenzhen, Xili, Nanshan, Shenzhen, Guangdong Province, P.R.China (zhangwl@sustc.edu.cn)

call our approach “convexification”.

3. We prove the existence and uniqueness of the minimizer of that functional on $B(m, R)$ and, most importantly, the *global convergence* of the gradient projection method to the correct solution of our CIP. In other words, the convergence of the gradient projection method to the correct solution is guaranteed if it starts from an arbitrary point of the set $B(m, R)$ and if the noise in the data tends to zero.
4. This theory is applied then to computational studies of the proposed numerical method. Such studies are not a part of [18].

We call a numerical method for a CIP *globally* convergent if a theorem is proved, which guarantees that this method delivers at least one point in a sufficiently small neighborhood of the exact solution without any advanced knowledge of this neighborhood. Thus, since the convergence to the exact solution of the gradient projection method of the minimization of the above mentioned weighted Tikhonov-like functional is guaranteed for any starting point of the set $B(m, R)$ and since its “size” $R > 0$ is an arbitrary number, then the numerical method proposed in this paper is a globally convergent one.

A conventional numerical methods for a CIP relies on the minimization of a Tikhonov least squares cost functional, see, e.g. [9, 12, 29, 33]. However, since, as a rule, such a functional is non convex, then the fundamental and still not addressed problem of such a method is the presence of multiple local minima and ravines in that functional. Therefore, convergence of an optimization method for such a functional can be guaranteed only if its starting point is located in a sufficiently small neighborhood of the exact solution, i.e. the *local* convergence. There exists a vast literature about numerical solutions of inverse scattering problems, which are close to the CIP we consider, see, e.g. [1, 2, 8, 11, 12, 13, 14, 15, 16, 31, 32, 29, 33] and references cited therein. They consider either problems of finding unknown coefficients or problems of finding shapes of obstacles. In the case of unknown coefficients, these cited papers consider the case of either multiple locations of the point source or multiple directions of the incident plane wave, which is unlike our case of a single point source.

Initially globally strictly convex cost functionals with CWFs in them were constructed in [17, 18, 19] for CIPs for hyperbolic and parabolic PDEs. Numerical studies were not conducted in these works. In the past few years an interest to this topic was renewed in publications of the first author with coauthors. New analytical results were combined with computational ones for some CIPs [23, 24, 25, 26, 28], including a quite challenging case of experimental data [27]. However, the convexification was not studied numerically for CIPs in time domain in the case when the initial condition is vanishing, as we have here. In the case of a non vanishing initial condition, a different version of the convexification was recently proposed in [4] for the PDE $u_{tt} = \Delta u + a(x)u$ with the unknown coefficient $a(x)$. The case of a non vanishing initial condition is less challenging one than our case of the δ -function in the initial condition. An indication of the latter is that the uniqueness theorem for the non vanishing case can be proved by the Bukhgeim-Klibanov method, which was originated in [7]. On the other hand, it is still unclear how to prove uniqueness theorem for our case of the δ -function in the initial condition. Thus, we just assume uniqueness here for computational purposes. Since this paper is not about the Bukhgeim-Klibanov method, we cite now, in addition to the above first publication, only some limited relevant references [5, 6, 20, 21].

In section 2 we state the CIP we consider. In section 3 we derive a boundary value problem for a system of coupled elliptic PDEs. In section 4 we derive the above

mentioned weighted globally strictly convex Tikhonov-like functional with a CWF in it and also formulate our Theorems 4.1-4.6. In section 5 we prove these theorems. In section 6 we present results of numerical experiments.

2. Statement of the Inverse Problem. Below $\mathbf{x} = (x, y, z) = (x_1, x_2, x_3) \in \mathbb{R}^3$. Let $A > 0$ be a number. Since the domain of interest Ω is a cube in our computations, then it is convenient to set $\Omega \subset \mathbb{R}^3$ as

$$(1) \quad \Omega = \{\mathbf{x} = (x, y, z) : -A/2 < x, y < A/2, z \in (0, A)\}.$$

Let the number $a > 0$. We set the single point source we use as $\mathbf{x}_0 = (0, 0, -a)$. Hence, this source is located below the domain Ω . Let Γ_0 be the upper boundary of Ω and Γ_1 be the rest of this boundary,

$$(2) \quad \Gamma_0 = \{\mathbf{x} = (x, y, z) : -A/2 < x, y < A/2, z = A\}, \Gamma_1 = \partial\Omega \setminus \Gamma_0.$$

Thus, Γ_0 is the “transmitted” side of Ω . Let the function $c(\mathbf{x})$ be such that

$$(3) \quad c \in C^{13}(\mathbb{R}^3),$$

$$(4) \quad c(\mathbf{x}) \geq c_0 = \text{const.} > 0 \text{ in } \overline{\Omega},$$

$$(5) \quad c(\mathbf{x}) = 1, \forall \mathbf{x} \in \mathbb{R}^3 \setminus \Omega.$$

Remark 2.1. We assume in (1) the C^{13} –smoothness of the function $c(\mathbf{x})$ since the representation (10) of the solution of the Cauchy problem (8), (9) works only under this assumption. Indeed, this smoothness was carefully calculated in Theorem 4.1 of the book [34].

The physical meaning of the function $c(\mathbf{x})$ is that $1/\sqrt{c(\mathbf{x})}$ is the speed of sound. Consider the conformal Riemannian metric generated by the function $c(\mathbf{x})$,

$$(6) \quad d\tau = \sqrt{c(\mathbf{x})} \sqrt{(dx)^2 + (dy)^2 + (dz)^2}.$$

The metric (6) generates geodesic lines $\Gamma(\mathbf{x}, \mathbf{x}_0)$, $\mathbf{x} \in \mathbb{R}^3$. Let $\tau(\mathbf{x})$ is the travel time along the geodesic line $\Gamma(\mathbf{x}, \mathbf{x}_0)$. Then [34] the function $\tau(\mathbf{x})$ is the solution of the eikonal equation

$$(7) \quad |\nabla \tau(\mathbf{x})|^2 = c(\mathbf{x}),$$

with the condition $\tau(\mathbf{x}) = O(|\mathbf{x} - \mathbf{x}_0|)$ as $|\mathbf{x} - \mathbf{x}_0| \rightarrow 0$. Furthermore,

$$\tau(\mathbf{x}) = \int_{\Gamma(\mathbf{x}, \mathbf{x}_0)} \sqrt{c(\mathbf{y})} d\sigma.$$

Everywhere below we rely on the following assumption without further comments [34]:

Regularity Assumption. For the above specific point source \mathbf{x}_0 , geodesic lines generated by the function $c(\mathbf{x})$ are regular. In other words, for any points $\mathbf{x} \in \mathbb{R}^3$ there exists unique geodesic line $\Gamma(\mathbf{x}, \mathbf{x}_0)$ connecting points \mathbf{x} and \mathbf{x}_0 .

A sufficient condition of the regularity of geodesic lines was derived in [35]. This condition is

$$\sum_{i,j=1}^3 \frac{\partial^2 \ln c(\mathbf{x})}{\partial x_i \partial x_j} \xi_i \xi_j \geq 0, \quad \forall \mathbf{x}, \xi \in \mathbb{R}^3.$$

As the forward problem, we consider the following Cauchy problem for the acoustic equation [10] of the hyperbolic type for the function $u(\mathbf{x}, \mathbf{x}_0, t)$:

$$(8) \quad c(\mathbf{x}) u_{tt} = \Delta u, \mathbf{x} \in \mathbb{R}^3, t > 0,$$

$$(9) \quad u(\mathbf{x}, 0) = 0, u_t(\mathbf{x}, 0) = \delta(\mathbf{x} - \mathbf{x}_0).$$

It was proven in Theorem 4.1 of [34] that, given the above conditions (3)-(5) as well as the Regularity Assumption, the problem (8), (9) has unique solution $u(\mathbf{x}, \mathbf{x}_0, t)$ which can be represented as

$$(10) \quad u(\mathbf{x}, t) = A(\mathbf{x}) \delta(t - \tau(\mathbf{x})) + H(t - \tau(\mathbf{x})) \hat{u}(\mathbf{x}, t),$$

where $\tau(\mathbf{x}), A(\mathbf{x}) \in C^{12}(\mathbb{R}^3)$, the function $\hat{u}(\mathbf{x}, t) \in C^2(t \geq \tau(\mathbf{x}))$ and $A(\mathbf{x}) > 0, \forall \mathbf{x} \in \mathbb{R}^3$. In (10) $H(z)$ is the Heaviside function,

$$H(z) = \begin{cases} 1, & z > 0, \\ 0, & z < 0. \end{cases}$$

Let the number $T > 0$. Denote $S_T = \partial\Omega \times (0, T)$ and $\Gamma_{0,T} = \Gamma_0 \times (0, T)$. Since we work with only a single location \mathbf{x}_0 of the point source, we will omit below indications of dependencies on \mathbf{x}_0 .

Coefficient Inverse Problem (CIP). *Let the domain Ω be as in (1). Suppose that the following two functions are given:*

$$(11) \quad u(\mathbf{x}, t) |_{(\mathbf{x}, t) \in S_T} = f_0(\mathbf{x}, t), \partial_z u(\mathbf{x}, t) |_{(\mathbf{x}, t) \in \Gamma_{0,T}} = f_1(\mathbf{x}, t),$$

Determine the function $c(\mathbf{x})$ for $\mathbf{x} \in \Omega$.

The knowledge of the normal derivative of the function $u(\mathbf{x}, t)$ at the upper boundary of the cube Ω can be justified as follows. Suppose that measurements $\varphi(x, y, t)$ of the amplitude $u(\mathbf{x}, t)$ of acoustic waves are conducted on the surface Γ_1 as well as on the plane $\{z = A\}$. Using (5), (8) and (9), we obtain in the half space $\{z > A\}$

$$u_{tt} = \Delta u, \mathbf{x} \in \{z > A\}, t > 0,$$

$$u(\mathbf{x}, 0) = u_t(\mathbf{x}, 0) = 0,$$

$$u(x, y, A) = \varphi(x, y, t), (x, y) \in \mathbb{R}^2, t > 0.$$

Solving this initial boundary value problem, we uniquely obtain the function $u(x, y, z, t)$ for $z > A, t > 0$. Next, we obtain $\partial_z u(x, y, A, t)$.

3. A System of Coupled Quasilinear Elliptic Equations. In this section we reduce the CIP (8)-(11) to the Cauchy problem for a system of coupled elliptic PDEs.

3.1. The function $w(\mathbf{x}, t)$. Integrate equation (8) twice with respect to t for points $\mathbf{x} \in \Omega$. Hence, we consider the function $p(\mathbf{x}, t)$,

$$(12) \quad p(\mathbf{x}, t) = \int_0^t dy \int_0^y u(\mathbf{x}, s) ds, \quad \mathbf{x} \in \Omega.$$

Hence, $p_{tt}(\mathbf{x}, t) = u(\mathbf{x}, t)$ for $\mathbf{x} \in \Omega$. Since $\mathbf{x}_0 \notin \overline{\Omega}$, then $\delta(\mathbf{x} - \mathbf{x}_0) = 0$ for $\mathbf{x} \in \Omega$. Hence, by (9)

$$(13) \quad \int_0^t dy \int_0^y u_{tt}(\mathbf{x}, s) ds = \int_0^t (u_t(\mathbf{x}, y) - u_t(\mathbf{x}, 0)) dy = u(\mathbf{x}, t) = p_{tt}(\mathbf{x}, t), \quad \mathbf{x} \in \Omega.$$

Next, by (8) and (12)

$$(14) \quad \int_0^t dy \int_0^y u_{tt}(\mathbf{x}, s) ds = \int_0^t dy \int_0^y \Delta u(\mathbf{x}, s) ds = \Delta p(\mathbf{x}, t), \quad \mathbf{x} \in \Omega.$$

Comparing (13) and (14), we obtain

$$(15) \quad p_{tt}(\mathbf{x}, t) = \Delta p(\mathbf{x}, t) \quad \text{for } (\mathbf{x}, t) \in \Omega \times (0, T).$$

Next, by (10) and (12)

$$(16) \quad p(\mathbf{x}, t) = A(\mathbf{x})(t - \tau(\mathbf{x}))H(t - \tau(\mathbf{x})) + O\left((t - \tau(\mathbf{x}))^2\right)H(t - \tau^0(\mathbf{x})),$$

where

$$(17) \quad \left| O\left((t - \tau(\mathbf{x}))^2\right) \right| \leq B(t - \tau(\mathbf{x}))^2 \quad \text{as } t \rightarrow \tau^+(\mathbf{x}),$$

$$(18) \quad \left| \partial_t O\left((t - \tau(\mathbf{x}))^2\right) \right| \leq B(t - \tau(\mathbf{x})) \quad \text{as } t \rightarrow \tau^+(\mathbf{x})$$

with a certain constant $B > 0$ independent on $(\mathbf{x}, t) \in \Omega \times (0, T)$.

Consider the function $w(\mathbf{x}, t)$ defined as

$$(19) \quad w(\mathbf{x}, t) = p(\mathbf{x}, t + \tau(\mathbf{x})), \quad \text{for } (\mathbf{x}, t) \in \Omega \times (0, T).$$

Then it follows from the above that $w \in C^2(\overline{\Omega} \times [0, T])$ and by (16)-(18)

$$(20) \quad w(\mathbf{x}, 0) = 0,$$

$$(21) \quad w_t(\mathbf{x}, 0) = A(\mathbf{x}) > 0.$$

Substituting (19) in (8) and using (7), we obtain

$$(22) \quad \Delta w - 2 \sum_{i=1}^3 w_{x_i t} \tau_{x_i} - w_t \Delta \tau = 0, \quad \mathbf{x} \in \Omega, t \in (0, T_1),$$

$$(23) \quad T_1 = T - \max_{\Omega} \tau(\mathbf{x}).$$

Denote $\tilde{f}_0(\mathbf{x}, t) = f_0(\mathbf{x}, t + \tau(\mathbf{x}))$ and $\tilde{f}_1(\mathbf{x}, t) = f_1(\mathbf{x}, t + \tau(\mathbf{x}))$. Then by (11)

$$(24) \quad w(\mathbf{x}, t) |_{(\mathbf{x}, t) \in S_{T_1}} = \tilde{f}_0(\mathbf{x}, t), \quad \partial_z w(\mathbf{x}, t) |_{(\mathbf{x}, t) \in \Gamma_{0, T_1}} = \tilde{f}_1(\mathbf{x}, t).$$

Thus, our goal below is to construct a numerical method, which would approximately find the functions $w(\mathbf{x}, t), \tau(\mathbf{x})$ for $\mathbf{x} \in \Omega, t \in (0, T_1)$ from conditions (20)-(24). Suppose that these two functions are approximated. Then the corresponding approximation for the target coefficient $c(\mathbf{x})$ can be easily found via the backwards calculation,

$$(25) \quad c(\mathbf{x}) = |\nabla \tau(\mathbf{x})|^2.$$

3.2. The system of coupled quasilinear elliptic PDEs. Lemma 3.1. *Consider the set of functions*

$$(26) \quad \{t, t^2, \dots, t^n, \dots\} = \{t^n\}_{n=1}^{\infty}.$$

Then this set is complete in $L_2(0, T_1)$.

Proof. Let a function $f(t) \in L_2(0, T_1)$ be such that

$$\int_0^{T_1} f(t) t^n dt = 0, n = 1, 2, \dots$$

Consider the function $\tilde{f}(t) = f(t)t$. Then

$$(27) \quad \int_0^{T_1} \tilde{f}(t) t^m dt = 0, m = 0, 1, 2, \dots$$

It is well known that (27) implies that $\tilde{f}(t) \equiv 0$. \square

Orthonormalize the set (26) using the Gram-Schmidt orthonormalization procedure. Then Lemma 3.1 implies that we obtain a basis $\{P_n(t)\}_{n=1}^{\infty}$ of orthonormal polynomials in $L_2(0, T_1)$ such that

$$(28) \quad P_n(0) = 0, \forall n = 1, 2, \dots$$

By (28) this is not a set of standard orthonormal polynomials.

Let the integer $N > 1$. Approximate the function $w(\mathbf{x}, t)$ as

$$(29) \quad w(\mathbf{x}, t) = \sum_{n=1}^N w_n(\mathbf{x}) P_n(t).$$

Here and below we use “=” instead of “ \approx ” for convenience. Substitute (29) in the left hand side of (22) and assume that the resulting left hand side equals zero. We obtain for $\mathbf{x} \in \Omega$

$$(30) \quad \sum_{n=1}^N \Delta w_n(\mathbf{x}) P_n(t) - 2 \sum_{i=1}^3 \tau_{x_i}(\mathbf{x}) \sum_{n=1}^N P'_n(t) \partial_{x_i} w_n(\mathbf{x}) - \Delta \tau(\mathbf{x}) \sum_{n=1}^N P'_n(t) w_n(\mathbf{x}) = 0.$$

By (21) and (29) we can assume that

$$(31) \quad \sum_{n=1}^N P'_n(0) w_n(\mathbf{x}) = A(\mathbf{x}) > 0, \quad \forall \mathbf{x} \in \bar{\Omega}.$$

Set in (??) $t = 0$. Hence, we obtain the first elliptic equation,

$$(32) \quad \Delta \tau(\mathbf{x}) + 2 \left[\sum_{i=1}^3 \tau_{x_i} \sum_{n=1}^N P'_n(0) \partial_{x_i} w_n(\mathbf{x}) \right] \left[\sum_{n=1}^N P'_n(0) w_n(\mathbf{x}) \right]^{-1} = 0, \quad \mathbf{x} \in \Omega.$$

We rewrite this equation as

$$(33) \quad \Delta \tau = F_1(\nabla \tau, \nabla \widetilde{W}, \widetilde{W}), \quad \mathbf{x} \in \Omega,$$

where $\widetilde{W}(x) = (w_1(\mathbf{x}), \dots, w_N(\mathbf{x}))^T$. Next, for $n = 1, \dots, N$ multiply both sides of (30) by $P_n(t)$ and integrate with respect to $t \in (0, T_1)$. Replace in the resulting equation $\Delta \tau$ with the right hand side of (33). We obtain

$$(34) \quad \Delta \widetilde{W} = F_2(\nabla \tau, \nabla \widetilde{W}, \widetilde{W}), \quad \mathbf{x} \in \Omega.$$

Consider the $(N + 1)$ -dimensional vector function

$$(35) \quad W(\mathbf{x}) = (\tau(\mathbf{x}), \widetilde{W}(\mathbf{x}))^T.$$

Thus, (24), (33) and (34) lead to the following Cauchy problem for a system of coupled quasilinear elliptic equations

$$(36) \quad \Delta W + F(\nabla W, W) = 0, \quad \mathbf{x} \in \Omega,$$

$$(37) \quad W|_{\partial\Omega} = q^0(\mathbf{x}), \quad \partial_z W|_{\Gamma_0} = q^1(\mathbf{x}),$$

$$(38) \quad q^0(\mathbf{x}) = (\tau(\mathbf{x}), q_1^0(\mathbf{x}), \dots, q_N^0(\mathbf{x}))^T, \quad q_n^0(\mathbf{x}) = \int_0^{T_1} \widetilde{f}_0(\mathbf{x}, t) P_n(t) dt, \quad \mathbf{x} \in \partial\Omega,$$

$$(39) \quad q^1(\mathbf{x}) = (\partial_z \tau(\mathbf{x}), q_1^1(\mathbf{x}), \dots, q_N^1(\mathbf{x}))^T, \quad q_n^1(\mathbf{x}) = \int_0^{T_1} \widetilde{f}_1(\mathbf{x}, t) P_n(t) dt, \quad \mathbf{x} \in \Gamma_0.$$

In (38) and (39) $n = 1, \dots, N$. In (36) the $(N + 1)$ -dimensional vector function $F \in C^1(\mathbb{R}^{3N+5})$. Thus, we have obtained the system (36) of coupled quasilinear elliptic PDEs with the Cauchy data (37)-(39). Unknowns in this problem are the function $\tau(\mathbf{x})$ and Fourier coefficients $w_n(\mathbf{x})$ of the function $w(\mathbf{x}, t)$ in (29). Therefore, we solve below the problem (36)-(39) of finding the $(N + 1)$ -dimensional vector function $W \in C^2(\bar{\Omega})$. In fact, however, we find below $W \in H^3(\Omega)$.

Remarks 3.1:

1. The number N in (29) should be chosen computationally, see section 6. Since (29) is an approximation of the function $w(\mathbf{x}, t)$, then (30)-(37) are also understood in the approximate sense. Thus, (29)-(37) form our **approximate mathematical model**. Since the original CIP is a very challenging one, it is hard to anticipate that it would be effectively solved numerically without such approximations. Since we develop a numerical method here, then it is fine to introduce an approximate mathematical model.
2. We cannot prove convergence of our resulting solutions to the correct one as $N \rightarrow \infty$. The underlying reason of this is the ill-posed nature of our CIP combined with the nonlinearity. On the other hand, truncated Fourier series are considered quite often in the field of Inverse and Ill-Posed Problems, whereas convergencies of resulting solutions at $N \rightarrow \infty$ are proven only very rarely. Nevertheless, corresponding approximate mathematical models usually provide quite good numerical results: we refer, e.g. to [15, 16, 26, 28] for corresponding publications.

4. Globally Strictly Convex Tikhonov-like Functional.

4.1. The functional. All Banach spaces considered below are spaces of real valued functions. If we say below that a vector function belongs to a certain Banach space, then this means that all its components belong to this space, and the norm of this function in that space is defined as the square root of the sum of squares of norms of its components.

To arrange a certain projection operator for the gradient projection method below, the best way is to have zero Cauchy data. Hence, we assume that there exists an $(N+1)$ -dimensional vector function $G = (g_0(\mathbf{x}), \dots, g_N(\mathbf{x}))^T \in H^3(\Omega)$ satisfying boundary conditions (37), i.e. such that

$$(40) \quad G|_{\partial\Omega} = q^0(\mathbf{x}), \partial_z G|_{\Gamma_0} = q^1(\mathbf{x}).$$

Let

$$(41) \quad W - G = Q \in H^3(\Omega), Q(\mathbf{x}) = (q_0(\mathbf{x}), \dots, q_N(\mathbf{x}))^T.$$

Then (36), (37) and (40) imply that

$$(42) \quad \Delta Q + \Delta G + F(Q + G, \nabla(Q + G)) = 0, \mathbf{x} \in \Omega,$$

$$(43) \quad Q|_{\partial\Omega} = 0, \partial_z Q|_{\Gamma_0} = 0.$$

Let $H_0^3(\Omega)$ be the subspace of the space $H^3(\Omega)$ defined as

$$H_0^3(\Omega) = \{v \in H^3(\Omega) : v|_{\partial\Omega} = 0, \partial_z v|_{\Gamma_0} = 0\}.$$

Choose an arbitrary number $R > 0$ and also choose another number $m \in (0, R)$, which is independent on R . Consider the set $B(m, R)$ of $(N+1)$ -dimensional vector functions $Z(\mathbf{x}) = (z_0(\mathbf{x}), \dots, z_N(\mathbf{x}))^T$ such that

$$(44) \quad B(m, R) = \left\{ \begin{array}{l} Z \in H_0^3(\Omega), \quad \|Z\|_{H^3(\Omega)} < R, \\ \sum_{n=1}^N P'_n(0)(z_n(\mathbf{x}) + g_n(\mathbf{x})) > m, \forall \mathbf{x} \in \bar{\Omega}. \end{array} \right.$$

The second condition (43) is generated by (31). By embedding theorem $H^3(\Omega) \subset C^1(\overline{\Omega})$. This implies that $\overline{B(m, R)} \subset C^1(\overline{\Omega})$ and also that there exist numbers $D_1(R) > 0$ and $D_2(G) > 0$ depending only on listed parameters such that

$$(45) \quad \|Z\|_{C^1(\overline{\Omega})} \leq D_1(R), \quad \forall Z \in \overline{B(m, R)},$$

$$(46) \quad \|G\|_{C^1(\overline{\Omega})} \leq D_2(G).$$

Temporary replace the vector functions $Q(\mathbf{x}) = (q_0(\mathbf{x}), \dots, q_N(\mathbf{x}))^T$ and $\nabla Q(\mathbf{x}) = (\nabla q_0(\mathbf{x}), \dots, \nabla q_N(\mathbf{x}))^T$ with the vector of real variables $(y_0, y_1, \dots, y_{4N+3})^T = y \in \mathbb{R}^{4N+4}$. Consider the set $Y \subset \mathbb{R}^{4N+4}$,

$$Y = \left\{ y \in \mathbb{R}^{4N+4} : \sum_{n=1}^N P'_n(0)(y_n + g_{n-1}(\mathbf{x})) > m, \forall \mathbf{x} \in \overline{\Omega} \right\}.$$

Obviously Y is an open set in \mathbb{R}^{4N+4} . Denote $p_1 = (y_0, \dots, y_N)$, $p_2 = (y_{0,1}, y_{0,2}, y_{0,3}, y_{1,1}, \dots, y_{N,3})$. Then $y = (p_1, p_2)^T \in \mathbb{R}^{4N+4}$. It follows from (32)-(36) that, as the function of y ,

$$(47) \quad F(p_1 + G(\mathbf{x}), p_2 + \nabla G(\mathbf{x})) \in C^2(\overline{Y}), \forall \mathbf{x} \in \overline{\Omega}.$$

Lemma 4.1. *The set $B(m, R)$ is convex.*

Proof. Let the number $\alpha \in (0, 1)$ and vector functions $Z, Y \in B(m, R)$. Consider the function $\alpha Z + (1 - \alpha)Y$. Then

$$\|\alpha Z + (1 - \alpha)Y\|_{H^3(\Omega)} \leq \alpha \|Z\|_{H^3(\Omega)} + (1 - \alpha)\|Y\|_{H^3(\Omega)} < \alpha R + (1 - \alpha)R = R.$$

Next, let $Z(\mathbf{x}) = (\tau_1(\mathbf{x}), z_1(\mathbf{x}), \dots, z_N(\mathbf{x}))^T$, $Y(\mathbf{x}) = (\tau_2(\mathbf{x}), y_1(\mathbf{x}), \dots, y_N(\mathbf{x}))^T$. Then

$$\alpha \sum_{n=1}^N P'_n(0)z_n(\mathbf{x}) + (1 - \alpha) \sum_{n=1}^N P'_n(0)y_n(\mathbf{x}) > \alpha m + (1 - \alpha)m = m. \quad \square$$

Our weighted Tikhonov-like cost functional is

$$(48) \quad J_{\lambda, \beta}(Q + G) = e^{-2\lambda b^2} \int_{\Omega} (\Delta Q + \Delta G + F(\nabla(Q + G), Q + G))^2 e^{2\lambda(z+b)^2} d\mathbf{x} \\ + \beta \|Q + G\|_{H^3(\Omega)}^2.$$

In (48) the numbers $\lambda \geq 1, b > 0, \beta \in (0, 1)$. Here, λ is the parameter of our CWF $e^{2\lambda(z+b)^2}$ and β is the regularization parameter. The multiplier $e^{-2\lambda b^2}$ is introduced to balance two terms in the right hand side of (48). Indeed, by (1)

$$(49) \quad \min_{\mathbf{x} \in \overline{\Omega}} \left(e^{-2\lambda b^2} e^{2\lambda(z+b)^2} \right) = 1.$$

Minimization Problem. *Minimize the functional $J_{\lambda, \beta}(Q)$ in (48) on the set $B(m, R)$ defined in (44).*

4.2. Theorems. Theorem 4.1. *There exists a sufficiently large number $\lambda_0 = \lambda_0(\Omega, b) \geq 1$ and a constant $C_1 = C_1(\Omega, b) > 0$, both depending only on Ω and b , such that for all $\lambda \geq \lambda_0$ and for all functions $u \in H^2(\Omega)$ such that $u|_{\partial\Omega} = u_z|_{\Gamma_0} = 0$ the following Carleman estimate holds*

$$(50) \quad \int_{\Omega} (\Delta u)^2 e^{2\lambda(z+b)^2} d\mathbf{x} \geq \frac{C_1}{\lambda} \sum_{i,j=1}^3 \int_{\Omega} u_{x_i x_j}^2 e^{2\lambda(z+b)^2} d\mathbf{x} \\ + C_1 \lambda \int_{\Omega} \left((\nabla u)^2 + \lambda^2 u^2 \right) e^{2\lambda(z+b)^2} d\mathbf{x}.$$

Below $C_2 = C_2(F, \|G\|_{H^3(\Omega)}, m, R, \Omega, b) > 0$ denotes different constants depending only on listed parameters.

Theorem 4.2 (global strict convexity). *For all $Q \in B(m, 2R)$, $\lambda, \beta > 0$ there exists Frechét derivative $J'_{\lambda, \beta}(Q + G) \in H_0^3(\Omega)$. Let λ_0 be the number of Theorem 4.1. There exists a number $\lambda_1 = \lambda_1(F, \|G\|_{H^3(\Omega)}, m, R, \Omega, b) \geq \lambda_0$ depending only on listed parameters such that for any $\lambda \geq \lambda_1$ and any $\beta > 0$ the functional $J_{\lambda, \beta}(Q)$ is strictly convex on $B(m, R)$, i.e. the following estimate holds for all $Q_1, Q_2 \in B(m, R)$*

$$(51) \quad J_{\lambda, \beta}(Q_2 + G) - J_{\lambda, \beta}(Q_1 + G) - J'_{\lambda, \beta}(Q_1 + G)(Q_2 - Q_1) \\ \geq \frac{C_2}{\lambda} \sum_{i,j=1}^3 \left\| (Q_2 - Q_1)_{x_i x_j} \right\|_{L_2(\Omega)}^2 + C_2 \lambda \|Q_2 - Q_1\|_{H^1(\Omega)}^2 + \beta \|Q_2 - Q_1\|_{H^3(\Omega)}^2.$$

Theorem 4.3. *The Frechét derivative $J'_{\lambda, \beta}(Q + G) \in H_0^3(\Omega)$ of the functional $J_{\lambda, \beta}(Q)$ satisfies the Lipschitz continuity condition in $B(m, 2R)$ for all $\lambda, \beta > 0$. In other words, there exists a number $L = L(F, \|G\|_{H^3(\Omega)}, m, R, \Omega, b, \lambda, \beta)$ depending only on listed parameters such that*

$$\left\| J'_{\lambda, \beta}(Q_2 + G) - J'_{\lambda, \beta}(Q_1 + G) \right\|_{H^3(\Omega)} \leq L \|Q_2 - Q_1\|_{H^3(\Omega)}, \quad \forall Q_1, Q_2 \in B(m, 2R).$$

Theorem 4.4. *For each pair $\lambda \geq \lambda_1, \beta > 0$ there exists unique minimizer $Q_{\min, \lambda, \beta} \in \overline{B(m, R)}$ of the functional $J_{\lambda, \beta}(Q)$ on the set $\overline{B(m, R)}$. Furthermore,*

$$(52) \quad J'_{\lambda, \beta}(Q_{\min, \lambda, \beta} + G)(Q_{\min, \lambda, \beta} - p) \leq 0, \quad \forall p \in H_0^3(\Omega).$$

We now arrange the gradient projection method of the minimization of the functional $J_{\lambda, \beta}(Q + G)$ on the set $\overline{B(m, R)}$. Let the number $\gamma \in (0, 1)$. Let $P_{\overline{B}} : H_0^3(\Omega) \rightarrow \overline{B(m, R)}$ be the projection operator of the space H_0^3 on the set $\overline{B(m, R)}$. Let $Q_0 \in B(m, R)$ be an arbitrary point of this set. The gradient projection method amounts to the following sequence:

$$(53) \quad Q_n = P_{\overline{B}}(Q_{n-1} - \gamma J'_{\lambda, \beta}(Q_{n-1} + G)), \quad n = 1, 2, \dots$$

Theorem 4.5. *Let λ_1 and β be parameters of Theorem 4.2. Choose a number $\lambda \geq \lambda_1$. Let $Q_{\min, \lambda, \beta} \in \overline{B(m, R)}$ be the unique minimizer of the functional $J_{\lambda, \beta}(Q)$ on the set $\overline{B(m, R)}$ (Theorem 4.3). Then there exists a sufficiently small number*

$\gamma_0 = \gamma_0 \left(F, \|G\|_{H^3(\Omega)}, m, R, \Omega, b, \beta \right) \in (0, 1)$ depending only on listed parameters such that the sequence (53) converges to $Q_{\min, \lambda, \beta}$ in the space $H^3(\Omega)$. More precisely, there exists a number $\theta = \theta \left(F, \|G\|_{H^3(\Omega)}, m, R, \Omega, b, \beta \right) \in (0, 1)$ such that the following estimate holds

$$(54) \quad \|Q_n - Q_{\min, \lambda, \beta}\|_{H^3(\Omega)} \leq \theta^n \|Q_{\min, \lambda, \beta} - Q_0\|_{H^3(\Omega)}.$$

Following the Tikhonov concept for ill-posed problems [5, 36], we now assume the existence of the exact solution $Q^*(\mathbf{x}) = (q_0^*(\mathbf{x}), \dots, q_N^*(\mathbf{x}))^T \in B(m, R)$ of the problem (42), (43) with the noiseless data $G^*(\mathbf{x}) = (g_0^*(\mathbf{x}), \dots, g_N^*(\mathbf{x}))^T \in H^3(\Omega)$. In particular, this means that

$$\sum_{n=1}^N P'_n(0) (q_n^*(\mathbf{x}) + g_n^*(\mathbf{x})) > m, \forall \mathbf{x} \in \bar{\Omega}.$$

Also, let the number $\delta \in (0, 1)$ be the level of the error in the data G , i.e.

$$(55) \quad \|G - G^*\|_{H^3(\Omega)} < \delta.$$

Since $\delta \in (0, 1)$, then (55) implies that we can regard in Theorem 4.6 that constants $\lambda_1, C_2, \gamma_0, \theta$ introduced above depend on $\|G^*\|_{H^3(\Omega)}$ rather than on $\|G\|_{H^3(\Omega)}$. We are doing so both in the formulation and in the proof of Theorem 4.6.

Theorem 4.6 (error estimates and convergence). *Let $\lambda_1 = \lambda_1 \left(F, \|G\|_{H^3(\Omega)}, m, R, \Omega, b \right)$ be the number of Theorem 4.2. Define the number η as $\eta = \left[4(A+b)^2 \right]^{-1}$. Choose a sufficiently small number $\delta_0 \in (0, 1)$ such that $\ln \delta_0^{-\eta} \geq \lambda_1$. Let in (55) $\delta \in (0, \delta_0)$. Choose $\lambda = \lambda(\delta) = \ln \delta^{-\eta} > \lambda_1$ implying that $\exp \left[2\lambda(\delta)(A+b)^2 \right] = 1/\sqrt{\delta}$. Let $Q_{\min, \lambda, \beta} \in \overline{B(m, R)}$ be the unique minimizer of the functional $J_{\lambda, \beta}(Q)$ on the set $\overline{B(m, R)}$, the existence of which is guaranteed by Theorem 4.4. Let $\{Q_n\}_{n=0}^\infty \subset \overline{B(m, R)}$ be the sequence of the gradient projection method (53) with an arbitrary starting point $Q_0 \in \overline{B(m, R)}$. Then the following estimates hold for all $\beta \in (0, 1)$*

$$(56) \quad \|Q^* - Q_{\min, \lambda, \beta}\|_{H^1(\Omega)} \leq C_2 \left(\delta^{\eta/2+1/4} + \sqrt{\beta} \delta^{\eta/2} \right),$$

$$(57) \quad \|Q^* - Q_{\min, \lambda, \beta}\|_{H^2(\Omega)} \leq C_2 \left(\delta^{1/4} + \sqrt{\beta} \right) \sqrt{\ln \delta^{-\eta}},$$

$$(58) \quad \|Q^* - Q_n\|_{H^1(\Omega)} \leq C_2 \left(\delta^{\eta/2+1/4} + \sqrt{\beta} \delta^{\eta/2} \right) + \theta^n \|Q_{\min, \lambda, \beta} - Q_0\|_{H^3(\Omega)},$$

$$(59) \quad \|Q^* - Q_n\|_{H^2(\Omega)} \leq C_2 \left(\delta^{1/4} + \sqrt{\beta} \right) \sqrt{\ln \delta^{-\eta}} + \theta^n \|Q_{\min, \lambda, \beta} - Q_0\|_{H^3(\Omega)},$$

$$(60) \quad \|c^* - c_n\|_{L_2(\Omega)} \leq C_2 \left(\delta^{1/4} + \sqrt{\beta} \right) \sqrt{\ln \delta^{-\eta}} + \theta^n \|Q_{\min, \lambda, \beta} - Q_0\|_{H^3(\Omega)},$$

In particular, if the regularization parameter $\beta = \sqrt{\delta}$, as required by the regularization theory [36], then estimates (56)-(59) become

$$\|Q^* - Q_{\min, \lambda, \beta}\|_{H^1(\Omega)} \leq C_2 \delta^{\eta/2+1/4}$$

$$\begin{aligned}
\|Q^* - Q_{\min,\lambda,\beta}\|_{H^2(\Omega)} &\leq C_2 \delta^{1/4} \sqrt{\ln \delta^{-\eta}}, \\
\|Q^* - Q_n\|_{H^1(\Omega)} &\leq C_2 \delta^{\eta/2+1/4} + \theta^n \left\| Q_{\min,\lambda,\sqrt{\delta}} - Q_0 \right\|_{H^3(\Omega)}, \\
\|Q^* - Q_n\|_{H^2(\Omega)} &\leq C_2 \delta^{1/4} \sqrt{\ln \delta^{-\eta}} + \theta^n \left\| Q_{\min,\lambda,\sqrt{\delta}} - Q_0 \right\|_{H^3(\Omega)}, \\
\|c^* - c_n\|_{L_2(\Omega)} &\leq C_2 \delta^{1/4} \sqrt{\ln \delta^{-\eta}} + \theta^n \left\| Q_{\min,\lambda,\sqrt{\delta}} - Q_0 \right\|_{H^3(\Omega)}.
\end{aligned}$$

Here $c_n(\mathbf{x})$ is defined via (41) with $Q = Q_n$, next (35), and next (25). Further, $c^*(\mathbf{x})$ is defined as the exact target coefficient, which corresponds to the noiseless data G^* with Q^* and $W^* = Q^* + G^*$ in (41), and next similarly as for $c_n(\mathbf{x})$.

Remarks 4.1:

1. The CWF of [18] depends on two large parameters, unlike the one in (48). This makes the CWF of [18] to be quite difficult for calculations, see a similar remark on page 1579 of [4] for the case of a CWF for the hyperbolic operator $\partial_t^2 - \Delta$. Thus, we establish in Theorem 4.1 a new Carleman estimate for the CWF $e^{2\lambda(z+b)^2}$.
2. It follows from (32)-(36) and (44) that condition (47) holds true.
3. Analogs of Theorems 4.3-4.6 were not proven in [18]. On the other hand, Theorems 4.4-4.6 are computationally oriented.
4. The regularization parameter β was not used in [18]. On the other hand, the presence of the regularization term $\beta \|Q + G\|_{H^3(\Omega)}^2$ in the functional $J_{\lambda,\beta}(Q + G)$ is important since this term ensures that in the gradient projection method (53) all functions $Q_n \in H_0^3(\Omega)$. Since $H^3(\Omega) \subset C^1(\overline{\Omega})$, and since we use estimates of $C^1(\overline{\Omega})$ -norms of some functions in the proof of Theorem 4.2, then we indeed need $Q_n \in H_0^3(\Omega)$. However, if using the functional of [18], then there is no guarantee that $Q_n \in H_0^3(\Omega)$. On the other hand, final estimates (56)-(59) are valid for all values $\beta \in (0, 1)$.

5. Proofs. We now refer to the publication [3] where some theorems of convex analysis are established. The proof of Theorem 4.3 is very similar with the proof of Theorem 3.1 of [3]. As soon as Theorems 4.2 and 4.3 are proven, the proof of Theorem 4.4 is quite similar with the proof of Lemma 2.1 of [3]. Next, as soon as Theorems 4.2 and 4.4 are proven, the proof of Theorem 4.5 is again quite similar with the proof of Theorem 2.1 of [3]. Hence, we prove here only Theorems 4.1, 4.2 and 4.6.

5.1. Proof of Theorem 4.1. In this proof, the function $u \in C^3(\overline{\Omega})$. The case $u \in H^2(\Omega)$ follows from density arguments. Consider the function $v = ue^{\lambda(z+b)^2}$. Then $u = ve^{-\lambda(z+b)^2}$. Hence, $u_{xx} = v_{xx}e^{-\lambda(z+b)^2}$, $u_{yy} = v_{yy}e^{-\lambda(z+b)^2}$,

$$u_{zz} = \left(v_{zz} - 2\lambda(z+b)v_z + 4\lambda^2(z+b)^2(1 + O(1/\lambda))v \right) e^{-\lambda(z+b)^2}.$$

In this proof, $C_1 = C_1(\Omega, b) > 0$ denotes different constants depending only on Ω and b and $O(1/\lambda)$ denotes different z -dependent functions satisfying $|O(1/\lambda)|, |\nabla O(1/\lambda)| \leq C_1/\lambda$. Hence,

$$\begin{aligned}
(\Delta u)^2 e^{2\lambda(z+b)^2} &= \left[\left(v_{xx} + v_{yy} + v_{zz} + 4\lambda^2(z+b)^2(1 + O(1/\lambda))v \right) - 2\lambda(z+b)v_z \right]^2 \\
&\geq -4\lambda(z+b)v_z \left(v_{xx} + v_{yy} + v_{zz} + 4\lambda^2(z+b)^2(1 + O(1/\lambda))v \right)
\end{aligned}$$

$$\begin{aligned}
&= (-4\lambda(z+b)v_zv_x)_x + 4\lambda(z+b)v_{zx}v_x + (-2\lambda(z+b)v_zv_y)_y + 4\lambda(z+b)v_{zy}v_y \\
&+ (-2\lambda(z+b)v_z^2)_z + 2\lambda v_z^2 + \left(-8\lambda^3(z+b)^3(1+O(1/\lambda))v^2\right)_z + 24\lambda^3(z+b)^3(1+O(1/\lambda))v^2 \\
&= -2\lambda(v_x^2 + v_y^2) + 2\lambda v_z^2 + 24\lambda^3(z+b)^3(1+O(1/\lambda))v^2 \\
&+ \left(-2\lambda(z+b)v_z^2 + 2\lambda(z+b)v_x^2 + 2\lambda(z+b)v_y^2 - 8\lambda^3(z+b)^3(1+O(1/\lambda))v^2\right)_z \\
&- 2\lambda(v_x^2 + v_y^2) + 2\lambda v_z^2 + 24\lambda^3(z+b)^2(1+O(1/\lambda))v^2.
\end{aligned}$$

Since $v|_{\partial\Omega} = v_z|_{\Gamma_0} = 0$ and $2\lambda v_z^2 \geq 0$, then integrating the above over Ω going back from v to u and using Gauss' formula, we obtain for sufficiently large $\lambda \geq C_1$

$$(61) \quad \int_{\Omega} (\Delta u)^2 e^{2\lambda(z+b)^2} d\mathbf{x} \geq -2\lambda \int_{\Omega} (u_x^2 + u_y^2)^2 e^{2\lambda(z+b)^2} d\mathbf{x} + 23\lambda^3 \int_{\Omega} u^2 e^{2\lambda(z+b)^2} d\mathbf{x}.$$

Next,

$$\begin{aligned}
-u\Delta u e^{2\lambda(z+b)^2} &= \left(-u_x u e^{2\lambda(z+b)^2}\right)_x + u_x^2 e^{2\lambda(z+b)^2} + \left(-u_y u e^{2\lambda(z+b)^2}\right)_y + u_y^2 e^{2\lambda(z+b)^2} \\
&+ \left(-u_z u e^{2\lambda(z+b)^2}\right)_z + u_z^2 e^{2\lambda(z+b)^2} + 4\lambda(z+b)u_z u e^{2\lambda(z+b)^2} \\
&= (u_x^2 + u_y^2 + u_z^2) e^{2\lambda(z+b)^2} + \left(2\lambda(z+b)u^2 e^{2\lambda(z+b)^2}\right)_z - 8\lambda^2(z+b)^2(1+O(1/\lambda))u^2 e^{2\lambda(z+b)^2} \\
&+ \left(-u_x u e^{2\lambda(z+b)^2}\right)_x + \left(-u_y u e^{2\lambda(z+b)^2}\right)_y.
\end{aligned}$$

Integrating this over Ω and using Gauss' formula, we obtain for sufficiently large $\lambda \geq C_1$

$$\begin{aligned}
(62) \quad & - \int_{\Omega} u\Delta u e^{2\lambda(z+b)^2} d\mathbf{x} = \int_{\Omega} (u_x^2 + u_y^2 + u_z^2) e^{2\lambda(z+b)^2} d\mathbf{x} \\
& - 9\lambda^2 \int_{\Omega} (z+b)^2 u^2 e^{2\lambda(z+b)^2} d\mathbf{x}.
\end{aligned}$$

Multiply (62) by $5\lambda/2$ and sum up with (61). Since $23\lambda^3 - (9 \cdot 5/2)\lambda^3 = \lambda^3/2$, then

$$\begin{aligned}
(63) \quad & -\frac{5}{2}\lambda \int_{\Omega} u\Delta u e^{2\lambda(z+b)^2} d\mathbf{x} + \int_{\Omega} (\Delta u)^2 e^{2\lambda(z+b)^2} d\mathbf{x} \\
& \geq \frac{1}{2}\lambda \int_{\Omega} (u_x^2 + u_y^2 + u_z^2) e^{2\lambda(z+b)^2} d\mathbf{x} + \frac{1}{2}\lambda^3 \int_{\Omega} u^2 e^{2\lambda(z+b)^2} d\mathbf{x}.
\end{aligned}$$

Next, applying Cauchy-Schwarz inequality, we obtain

$$-\frac{5}{2}\lambda \int_{\Omega} u\Delta u e^{2\lambda(z+b)^2} d\mathbf{x} + \int_{\Omega} (\Delta u)^2 e^{2\lambda(z+b)^2} d\mathbf{x} \leq \frac{25}{4}\lambda^2 \int_{\Omega} u^2 e^{2\lambda(z+b)^2} d\mathbf{x} + \frac{1}{2} \int_{\Omega} (\Delta u)^2 e^{2\lambda(z+b)^2} d\mathbf{x}.$$

Combining this with (63), we obtain for sufficiently large $\lambda_0 = \lambda_0(\Omega, b) > 0$ and for $\lambda \geq \lambda_0$

$$(64) \quad \int_{\Omega} (\Delta u)^2 e^{2\lambda(z+b)^2} d\mathbf{x} \geq C_1 \lambda \int_{\Omega} \left((\nabla u)^2 + \lambda^2 u^2 \right) e^{2\lambda(z+b)^2} d\mathbf{x}.$$

The next step is to incorporate the term with second derivatives in (50). We have

$$(65) \quad (\Delta u)^2 e^{2\lambda(z+b)^2} = (u_{xx} + u_{yy} + u_{zz})^2 e^{2\lambda(z+b)^2} = (u_{xx}^2 + u_{yy}^2 + u_{zz}^2) e^{2\lambda(z+b)^2} \\ + 2(u_{xx}u_{yy} + u_{xx}u_{zz} + u_{yy}u_{zz}) e^{2\lambda(z+b)^2}.$$

The second line of (50) gives:

$$(66) \quad (2u_{xx}u_{yy} + 2u_{xx}u_{zz} + 2u_{yy}u_{zz}) e^{2\lambda(z+b)^2} = \left(2u_{xx}u_y e^{2\lambda(z+b)^2} \right)_y - 2u_{xy}u_y e^{2\lambda(z+b)^2} \\ + \left(2u_{xx}u_z e^{2\lambda(z+b)^2} \right)_z - 2u_{xz}u_z e^{2\lambda(z+b)^2} - 8\lambda(z+b)u_{xx}u_z e^{2\lambda(z+b)^2} \\ + \left(2u_{yy}u_z e^{2\lambda(z+b)^2} \right)_z - 2u_{yz}u_z e^{2\lambda(z+b)^2} - 8\lambda(z+b)u_{yy}u_z e^{2\lambda(z+b)^2} \\ = 2(u_{xy}^2 + u_{xz}^2 + u_{yz}^2) e^{2\lambda(z+b)^2} + \left[2(u_{xy}u_y - u_{xz}u_z) e^{2\lambda(z+b)^2} \right]_x \\ + \left[2(u_{xx}u_y - u_{xz}u_z) e^{2\lambda(z+b)^2} \right]_y - 8\lambda(z+b)u_{xx}u_z e^{2\lambda(z+b)^2} - 8\lambda(z+b)u_{yy}u_z e^{2\lambda(z+b)^2}.$$

Using Cauchy-Schwarz inequality, we estimate from the below the last line of (66) as

$$(67) \quad -8\lambda(z+b)u_{xx}u_z e^{2\lambda(z+b)^2} - 8\lambda(z+b)u_{yy}u_z e^{2\lambda(z+b)^2} \\ \geq -\frac{1}{2}(u_{xx}^2 + u_{yy}^2) e^{2\lambda(z+b)^2} - 64\lambda^2(z+b)^2 u_z^2 e^{2\lambda(z+b)^2}.$$

Combining (66)-(67), we obtain

$$\int_{\Omega} (\Delta u)^2 e^{2\lambda(z+b)^2} d\mathbf{x} \geq \frac{1}{2} \sum_{i,j=1}^3 \int_{\Omega} u_{x_i x_j}^2 e^{2\lambda(z+b)^2} d\mathbf{x} - 64\lambda^2 \int_{\Omega} (z+b)^2 u_z^2 e^{2\lambda(z+b)^2} d\mathbf{x}.$$

Multiply this estimate by $C_1/(128\lambda)$ and sum up with (64). We obtain

$$(68) \quad \left(1 + \frac{C_1}{128\lambda} \right) \int_{\Omega} (\Delta u)^2 e^{2\lambda(z+b)^2} d\mathbf{x} \geq \frac{C_1}{256\lambda} \sum_{i,j=1}^3 \int_{\Omega} u_{x_i x_j}^2 e^{2\lambda(z+b)^2} d\mathbf{x} \\ + \frac{C}{2} \lambda \int_{\Omega} \left((\nabla u)^2 + \lambda^2 u^2 \right) e^{2\lambda(z+b)^2} d\mathbf{x}.$$

Since $C_1 > 0$ denotes different constants, then the target estimate (50) follows from (52) immediately. \square

5.2. Proof of Theorem 4.2. Denote $h = Q_2 - Q_1$ implying that $Q_2 = Q_1 + h$. Also, $h \in H_0^3(\Omega)$, $\|h\|_{H^3(\Omega)} < 2R$. Hence, by (45)

$$(69) \quad \|h\|_{C^1(\overline{\Omega})} < D_1(2R).$$

Using the multidimensional analog of Taylor formula (see, e.g. [37] for this formula) and (47), we obtain

$$(70) \quad \begin{aligned} & \Delta h + (\Delta Q_1 + \Delta G) + F(h + Q_1 + G, \nabla(h + Q_1 + G)) \\ &= \left[\Delta h + F^{(1)}(Q_1 + G, \nabla(Q_1 + G))h + F^{(2)}(Q_1 + G, \nabla(Q_1 + G))\nabla h \right] \\ &+ F_{nonlin}(h, \nabla h, Q_1 + G, \nabla(Q_1 + G)) + [(\Delta Q_1 + \Delta G) + F(Q_1 + G, \nabla(Q_1 + G))], \end{aligned}$$

where elements of $(N+1) \times (N+1)$ matrix $F^{(1)}$ and $(3N+3) \times (3N+3)$ matrix are bounded for $\mathbf{x} \in \overline{\Omega}$, i.e.

$$(71) \quad \left| F_{i,j}^{(1)}(Q_1 + G, \nabla(Q_1 + G)) \right|, \left| F_{i,j}^{(2)}(Q_1 + G, \nabla(Q_1 + G)) \right| \leq C_2, \quad \forall \mathbf{x} \in \overline{\Omega},$$

where the subscript “ i, j ” denotes an arbitrary element of the corresponding matrix indexed as (i, j) . Next, the $(N+1)$ -dimensional vector function F_{nonlin} depends nonlinearly on $h, \nabla h$. Furthermore, the following estimate follows from (45)-(47)

$$(72) \quad |F_{nonlin}(h, \nabla h, Q_1 + G, \nabla(Q_1 + G))| \leq C_2 \left(|h|^2 + |\nabla h|^2 \right), \quad \forall \mathbf{x} \in \overline{\Omega}.$$

Next, (69) and (72) imply with a different constant C_2

$$(73) \quad |F_{nonlin}(h, \nabla h, Q_1 + G, \nabla(Q_1 + G))| \leq C_2 (|h| + |\nabla h|), \quad \forall \mathbf{x} \in \overline{\Omega}.$$

It follows from (70)-(73) that

$$(74) \quad \begin{aligned} & [\Delta h + (\Delta Q_1 + \Delta G) + F(h + Q_1 + G, \nabla(h + Q_1 + G))]^2 \\ &= [(\Delta Q_1 + \Delta G) + F(Q_1 + G, \nabla(Q_1 + G))]^2 \\ &+ Lin_1(\Delta h) + Lin_2(\nabla h) + Lin_3(h) \\ &+ (\Delta h)^2 + M_1(h, \nabla h, Q_1 + G, \nabla(Q_1 + G))\Delta h + M_2(h, \nabla h, Q_1 + G, \nabla(Q_1 + G)), \end{aligned}$$

where expressions $Lin_1(\Delta h)$, $Lin_2(\nabla h)$ and $Lin_3(h)$ are linear with respect to $\Delta h, \nabla h$ and h respectively and

$$(75) \quad |Lin_1(\Delta h) + Lin_2(\nabla h) + Lin_3(h)| \leq C_2 (|\Delta h| + |\nabla h| + |h|), \quad \forall \mathbf{x} \in \overline{\Omega}.$$

Next, the following estimates are valid for M_1 and M_2

$$(76) \quad |M_1(h, \nabla h, Q_1 + G, \nabla(Q_1 + G))| \leq C_2 (|\nabla h| + |h|), \quad \forall \mathbf{x} \in \overline{\Omega},$$

$$(77) \quad |M_2(h, \nabla h, Q_1 + G, \nabla(Q_1 + G))| \leq C_2 (|\nabla h|^2 + |h|^2), \quad \forall \mathbf{x} \in \overline{\Omega}.$$

In particular, (76), (77) and Cauchy-Schwarz inequality imply

$$(78) \quad \begin{aligned} & (\Delta h)^2 + M_1 (h, \nabla h, Q_1 + G, \nabla (Q_1 + G)) \Delta h + M_2 (h, \nabla h, Q_1 + G, \nabla (Q_1 + G)) \\ & \geq \frac{1}{2} (\Delta h)^2 - C_2 (|\nabla h|^2 + |h|^2), \forall \mathbf{x} \in \bar{\Omega}. \end{aligned}$$

Using (48) and (74)-(77), we obtain

$$(79) \quad J_{\lambda, \beta} (Q_1 + h) - J_{\lambda, \beta} (Q_1) = X_{lin} (h) + X_{nonlin} (h),$$

where $X_{lin} (h)$ can be extended from $\left\{ \|h\|_{H^3(\Omega)} < 2R \right\} \subset H_0^3 (\Omega)$ to the entire space $H^3 (\Omega)$ as a bounded linear functional,

$$(80) \quad X_{lin} (h) = e^{-2\lambda b^2} \int_{\Omega} (Lin_1 (\Delta h) + Lin_2 (\nabla h) + Lin_3 (h)) (\mathbf{x}) e^{2\lambda(z+b)^2} d\mathbf{x} + 2\beta [h, Q_1 + G],$$

where $[.,.]$ is the scalar product in $H^3 (\Omega)$. As to $X_{nonlin} (h)$ in (79), it follows from (48), (74), (76) and (77) that

$$(81) \quad \lim_{\|h\|_{H^3(\Omega)} \rightarrow 0} \frac{X_{nonlin} (h)}{\|h\|_{H^3(\Omega)}} = 0.$$

Using (75) and (79)-(81), we obtain that $X_{lin} (h)$ is the Frechét derivative $J'_{\lambda, \beta} (Q)$ of the functional $J_{\lambda, \beta} (Q)$ at the point Q , i.e. $X_{lin} (h) = J'_{\lambda, \beta} (Q_1) (h)$. Thus, the existence of the Frechét derivative is established.

Next, using (48) and (74)-(80), we obtain

$$(82) \quad \begin{aligned} & J_{\lambda, \beta} (Q_1 + G + h) - J_{\lambda, \beta} (Q_1 + G) - J'_{\lambda, \beta} (Q_1 + G) (h) \\ & \geq \frac{1}{2} e^{-2\lambda b^2} \int_{\Omega} (\Delta h)^2 e^{2\lambda(z+b)^2} d\mathbf{x} - C_2 e^{-2\lambda b^2} \int_{\Omega} (|\nabla h|^2 + |h|^2) e^{2\lambda(z+b)^2} d\mathbf{x} + \beta \|h\|_{H^3(\Omega)}^2. \end{aligned}$$

We now apply Carleman estimate (50), assuming that $\lambda \geq \lambda_0$,

$$\begin{aligned} & \frac{1}{2} e^{-2\lambda b^2} \int_{\Omega} (\Delta h)^2 e^{2\lambda(z+b)^2} d\mathbf{x} - C_2 e^{-2\lambda b^2} \int_{\Omega} (|\nabla h|^2 + |h|^2) e^{2\lambda(z+b)^2} d\mathbf{x} + \beta \|h\|_{H^3(\Omega)}^2 \\ & \geq \frac{C_1}{\lambda} \sum_{i,j=1}^3 e^{-2\lambda b^2} \int_{\Omega} h_{x_i x_j}^2 e^{2\lambda(z+b)^2} d\mathbf{x} + C_1 \lambda e^{-2\lambda b^2} \int_{\Omega} ((\nabla h)^2 + \lambda^2 h^2) e^{2\lambda(z+b)^2} d\mathbf{x} \\ & \quad - C_2 e^{-2\lambda b^2} \int_{\Omega} (|\nabla h|^2 + |h|^2) e^{2\lambda(z+b)^2} d\mathbf{x} + \beta \|h\|_{H^3(\Omega)}^2. \end{aligned}$$

Choosing sufficiently large $\lambda_1 = \lambda_1 (F, \|G\|_{H^3(\Omega)}, m, R, \Omega, b) \geq \lambda_0$ and letting $\lambda \geq \lambda_1$, we obtain with a different constant C_2

$$\begin{aligned} & \frac{1}{2} e^{-2\lambda b^2} \int_{\Omega} (\Delta h)^2 e^{2\lambda(z+b)^2} d\mathbf{x} - C_2 e^{-2\lambda b^2} \int_{\Omega} (|\nabla h|^2 + |h|^2) e^{2\lambda(z+b)^2} d\mathbf{x} + \beta \|h\|_{H^3(\Omega)}^2 \\ & \geq \frac{C_2}{\lambda} \sum_{i,j=1}^3 e^{-2\lambda b^2} \int_{\Omega} h_{x_i x_j}^2 e^{2\lambda(z+b)^2} d\mathbf{x} + C_2 \lambda e^{-2\lambda b^2} \int_{\Omega} ((\nabla h)^2 + \lambda^2 h^2) e^{2\lambda(z+b)^2} d\mathbf{x} + \beta \|h\|_{H^3(\Omega)}^2. \end{aligned}$$

This, (82) and (49) imply (51). \square

5.3. Proof of Theorem 4.6. We rewrite the functional $J_{\lambda,\beta}(Q)$ in (48) as

$$(83) \quad J_{\lambda,\beta}(Q + G) = J_{\lambda,\beta}^0(Q + G) + \beta \|Q + G\|_{H^3(\Omega)}^2.$$

Since the vector function $Q^* \in B(m, R)$ is the exact solution of the problem (42), (43) with the noiseless data G^* , then $J_{\lambda,\beta}^0(Q^* + G^*) = 0$. Hence,

$$(84) \quad J_{\lambda,\beta}(Q^* + G^*) \leq C_2\beta.$$

Next, $J_{\lambda,\beta}(Q^* + G) = (J_{\lambda,\beta}(Q^* + G) - J_{\lambda,\beta}(Q^* + G^*)) + J_{\lambda,\beta}(Q^* + G^*)$. Hence, applying (84), we obtain

$$(85) \quad J_{\lambda,\beta}(Q^* + G) \leq |J_{\lambda,\beta}(Q^* + G) - J_{\lambda,\beta}(Q^* + G^*)| + C_2\beta.$$

Using (55) and (83), we estimate the first term in the right hand side of (85),

$$(86) \quad \begin{aligned} |J_{\lambda,\beta}(Q^* + G) - J_{\lambda,\beta}(Q^* + G^*)| &\leq |J_{\lambda,\beta}^0(Q^* + G) - J_{\lambda,\beta}^0(Q^* + G^*)| + C_2\beta\delta \\ &\leq C_2\delta \exp\left(2\lambda(A+b)^2\right) + C_2\beta\delta. \end{aligned}$$

Recall that due to our choice $\lambda = \lambda(\delta) = \ln \delta^{-\eta}$, where $\eta = \left[4(A+b)^2\right]^{-1}$, we have $\delta \exp\left(2\lambda(A+b)^2\right) = 1/\sqrt{\delta}$. Hence, (86) implies

$$|J_{\lambda,\beta}(Q^* + G) - J_{\lambda,\beta}(Q^* + G^*)| \leq C_2\sqrt{\delta}, \quad \forall \beta \in (0, 1).$$

Combining this with (84), we obtain

$$(87) \quad J_{\lambda,\beta}(Q^* + G) \leq C_2\left(\sqrt{\delta} + \beta\right).$$

Until now we have not used in this proof the strict convexity of the functional $J_{\lambda,\beta}(Q + G)$ for $Q \in B(m, R)$. But we will use this property in the rest of the proof. Recall that by Theorem 4.3 $Q_{\min,\lambda,\beta} \in \overline{B(m, R)}$ is the unique minimizer on the set $\overline{B(m, R)}$ of the functional $J_{\lambda,\beta}(Q + G)$ on the set $\overline{B(m, R)}$. By Theorem 4.2

$$(88) \quad \begin{aligned} &J_{\lambda,\beta}(Q^* + G) - J_{\lambda,\beta}(Q_{\min,\lambda,\beta} + G) - J'_{\lambda,\beta}(Q_{\min,\lambda,\beta})(Q^* - Q_{\min,\lambda,\beta}) \\ &\geq \frac{C_2}{\lambda} \sum_{i,j=1} \left\| (Q^* - Q_{\min,\lambda,\beta})_{x_i x_j} \right\|_{L_2(\Omega)}^2 + C_2\lambda \|Q^* - Q_{\min,\lambda,\beta}\|_{H^1(\Omega)}^2 + \frac{\beta}{2} \|Q^* - Q_{\min,\lambda,\beta}\|_{H^3(\Omega)}^2. \end{aligned}$$

Since by (52) $-J'_{\lambda,\beta}(Q_{\min,\lambda,\beta})(Q^* - Q_{\min,\lambda,\beta}) \leq 0$, then (87) implies that the left hand side of (88) can be estimated as

$$J_{\lambda,\beta}(Q^* + G) - J_{\lambda,\beta}(Q_{\min,\lambda,\beta} + G) - J'_{\lambda,\beta}(Q_{\min,\lambda,\beta} + G)(Q^* - Q_{\min,\lambda,\beta}) \leq C_2\left(\sqrt{\delta} + \beta\right).$$

Hence, using our choice of $\lambda = \lambda(\delta) = \ln \delta^{-\eta}$ and (88), we obtain estimates (56) and (57). Estimates (58) and (59) are obtained from (56) and (57) respectively using (54) and the triangle inequality. Estimate (60) obviously follows from estimate (59). \square

6. Numerical Studies. The single point source is now $\mathbf{x}_0 = (0, 0, -5)$. We choose in (1) the numbers $A = 1$. Hence, below

$$\Omega = \{-1/2 < x, y < 1/2, z \in (0, 1)\},$$

$$(89) \quad \Gamma_0 = \{\mathbf{x} = (x, y, z) : -1/2 < x, y < 1/2, z = 1\}, \Gamma_1 = \partial\Omega \setminus \Gamma_0.$$

We have introduced the vector function G in section 4.1 and thus obtained the problem (42), (43) for the vector function $Q = W - G$ from the problem (36), (37) for the vector function W in order to obtain zero boundary conditions (43) for Q . The latter was convenient for proofs of Theorems 4.3-4.6. However, it follows from Theorems 4.2-4.6 that their obvious analogs hold true for the functional

$$(90) \quad J_{\lambda, \beta}(W) = e^{-2\lambda b^2} \int_{\Omega} (\Delta W + F(\nabla W, W))^2 e^{2\lambda(z+b)^2} d\mathbf{x} + \beta \|W\|_{H^3(\Omega)}^2,$$

$$(91) \quad W \in B_W(m, R) = \{W : W = Q - G, \forall Q \in B(m, R)\}.$$

Furthermore, we use in (90) $\beta = 0, b = 0$. Therefore, we ignore the multiplier $e^{-2\lambda b^2}$, which was used above to balance first and second terms in the right hand side of (48), see (49). Hence, we minimize the weighted cost functional

$$(92) \quad J_{\lambda}(W) = \int_{\Omega} (\Delta W + F(\nabla W, W))^2 e^{2\lambda z^2} d\mathbf{x}$$

on the set (91). We conjecture that the case $\beta = 0$ works probably because the minimal mesh size of $1/32$ in the finite differences we use to minimize this functional is not too small, and all norms in finite dimensional spaces are equivalent, see item 4 of Remark 4.1. In addition, recall that, by the same item, one can choose any value of $\beta \in (0, 1)$ in convergence estimates (56)-(59). Also, we use the gradient descent method (GD) instead of a more complicated gradient projection method. We have observed that GD works well for our computations. The latter coincides with observations in all earlier publications about numerical studies of the convexification [23, 24, 25, 26, 27, 28]. As to our choice $b = 0$, one can derive from the proof of Theorem 4.1 that a slightly modified Carleman estimate of this theorem works in a little bit smaller domain $\Omega' = \Omega \cap \{z > \varepsilon\}$ for any small number $\varepsilon > 0$. Finally, we believe that simplifications listed in this section work well numerically due to a commonly known observation that numerical studies are usually less pessimistic than the theory is.

6.1. Some details of the numerical implementation. To solve the inverse problem, we should first computationally simulate the data (11) at $\partial\Omega$ via the numerical solution of the forward problem (8), (9). To solve the problem (8), (9) computationally, we have used the standard finite difference method. To avoid the use of the infinite space \mathbb{R}^3 in the solution of the forward problem, we choose the cube $\Omega_f = \{-6.5 < x, y < 6.5, z \in (-6, 7)\}$. So that $\Omega \subset \Omega_f$, $\partial\Omega \cap \partial\Omega_f = \emptyset$ and $\mathbf{x}_0 = (0, 0, -5) \in \Omega_f$. We choose a sufficiently large number $T_0 = 6.5$. Then we solve equation (8) with the initial condition (9) and zero Dirichlet boundary condition at $\partial\Omega_f$ for $(\mathbf{x}, t) \in \Omega_f \times (0, T_0)$ via finite differences. Indeed, the wave originated at \mathbf{x}_0

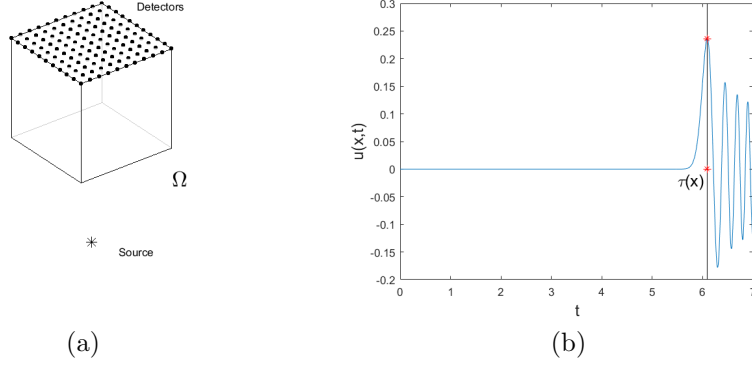


FIG. 1. (a) A schematic diagram of domains Ω , source and detectors. (b) This figure explains how do we approximately choose the boundary condition $\tau(\mathbf{x})|_{\partial\Omega}$. We have chosen here a selected point $\mathbf{x} \in \Gamma_0$

cannot reach neither vertical sides of Ω_f nor the upper side $\{z = 7\} \cap \overline{\Omega_f}$ of Ω for times $t \in (0, 6.5)$. However, it reaches the upper side $\{z = 1\} \cap \overline{\Omega}$ of Ω at $t = 6$. This wave reaches the lower side $\{z = -6\} \cap \overline{\Omega_f}$ of Ω_f at $t = 1$, which means that the zero Dirichlet boundary condition on the lower side is incorrect. Still, for $t \in (0, 6.5)$, the wave reflected from the lower side of Ω_f does not reach the upper side $\{z = 1\} \cap \overline{\Omega}$ of Ω , where the data for our CIP are given. Hence, this reflected wave does not affect our data.

We use the explicit scheme. The grid step size in each spatial direction is $\Delta x = 1/32$ and in time direction $\Delta t = 0.002$. To avoid a substantial increase of the computational time, we do not decrease these step sizes. When solving the forward problem, we model the $\delta(\mathbf{x} - \mathbf{x}_0)$ -function in (9) as

$$\tilde{\delta}(\mathbf{x} - \mathbf{x}_0) = \begin{cases} \frac{1}{\varepsilon} \exp\left(-\frac{1}{1-|\mathbf{x}-\mathbf{x}_0|^2/\varepsilon}\right), & \text{if } |\mathbf{x} - \mathbf{x}_0|^2 < \varepsilon = 0.01, \\ 0, & \text{otherwise.} \end{cases}$$

In computations of the inverse problem, for each test we use, we choose in the data (11) $T = \max_{\overline{\Omega}} \tau(\mathbf{x}) + 0.1$. We have observed that $T < T_0$ in all our tests. Next, we set $T_1 = T - \max_{\overline{\Omega}} \tau(\mathbf{x}) = 0.1$, see (22), (23). An important question is on how do we figure out boundary conditions at $\partial\Omega$ for the function $\tau(\mathbf{x})$, i.e. $\tau(\mathbf{x})|_{\partial\Omega}$ and also $\partial_z \tau(\mathbf{x})|_{\Gamma_0}$. In principle, for $\mathbf{x} \in \partial\Omega$, one should choose such a number $\tau_0(\mathbf{x})$ that $\tau_0(\mathbf{x}) = \min_t \{t : u(\mathbf{x}, t) > 0\}$. However, it is hard to choose in practice the number $\tau_0(\mathbf{x})$ satisfying this criterion. Therefore, we calculate such a number $\tilde{t}(\mathbf{x})$ at which the first wave with the largest maximal value arrives at the point $\mathbf{x} \in \partial\Omega$, see Figure 2. Next, we set $\tau_0(\mathbf{x})|_{\partial\Omega} := \tilde{t}(\mathbf{x})|_{\partial\Omega}$. To calculate the derivative $\partial_z \tau_0(\mathbf{x})|_{\Gamma_0}$, we compute the discrete normal derivative of $\tau_0(\mathbf{x})$ over the mesh in the forward problem.

To minimize the weighted cost functional $J_\lambda(W)$ in (91), we act similarly with the previous above cited works about numerical studies of the convexification for a number of other CIPs. More precisely, we write the differential operators involved in $J_\lambda(W)$ via finite differences and minimize with respect to the values of the discrete analog of the vector function W at grid points. As to the choice of the parameter λ , even though the above theory works only for sufficiently large values of λ , we have established in our computational experiments that the choice $\lambda = 1$ is an optimal one for all tests we have performed. This again repeats observation of all above cited works

on numerical studies of the convexification, in which the optimal choice was $\lambda \in [1, 3]$. We have also tested two different values of the number N terms in the series (29): $N = 1$ and $N = 3$. Our computational results indicate that $N = 3$ provides results of a good quality. In all tests below, the starting point of GD is the vector function $W(\mathbf{x})$, which is generated by the coefficient $c(\mathbf{x}) \equiv 1$ in equation (8), $W_{c \equiv 1}(\mathbf{x})$.

6.2. A multi-level minimization method of the functional $J_\lambda(W)$. We have found in our computational experiments that the gradient descent method for our weighted cost functional $J_{\lambda,0}(W)$ converges rapidly on a coarse mesh. This provides us with a rough image. Hence, we have implemented a multi-level method [30]. Let $M_{h_1} \subset M_{h_2} \dots \subset M_{h_K}$ be nested finite difference meshes, i.e. M_{h_k} is a refinement of $M_{h_{k-1}}$ for $k \leq K$. Let P_{h_k} be the corresponding finite difference functional space. On the first level M_{h_1} , we solve the discrete optimization problem. In other words, let $W_{h_1,\min}$ be the minimizer on the finite difference analog of the set (91) of the following functional

$$(93) \quad J_\lambda(W_{h_1}) = \int_{\Omega} (\Delta W_{h_1} + F(\nabla W_{h_1}, W_{h_1}))^2 e^{2\lambda z^2} d\mathbf{x}.$$

In (93) the integral and the derivatives are understood in the discrete sense, and $W_{h_1,\min}$ is found via the GD. Then we interpolate the minimizer $W_{h_1,\min}$ on the finer mesh M_{h_2} and use the resulting vector function $W_{h_2,\text{int}}$ as the starting point of the gradient descent method of the optimization of the direct analog of functional (93) in which h_1 is replaced with h_2 and W_{h_1} is replaced with W_{h_2} . This process is repeated until we obtain the minimizer $W_{h_K,\min}$ on the K_{th} level on the mesh M_{h_K} .

Since $(x, y, z) \in (-1/2, 1/2) \times (-1/2, 1/2) \times (0, 1)$, then our first level M_{h_1} is set to be the uniform mesh with the grid step $h_1 = 1/8$. For each mesh refinement, we will refine the mesh via setting the new grid step of the refined mesh in all directions to be $1/2$ of the previous grid step. On each level M_{h_k} , we stop iterations as soon as we see that $\|\nabla J_\lambda^{(h_k)}(W_{h_k})\| < 2 \times 10^{-2}$. Next, we refine the mesh and compute the solution on the next level $M_{h_{k+1}}$. In the end, we compute our approximation for the target coefficient $c(\mathbf{x})$ using the final minimizer $W_{h_K,\min}$.

6.3. Numerical testing. In the tests of this section, we demonstrate the efficiency of our numerical method for imaging of small inclusions as well as for imaging of a smoothly varying function $c(\mathbf{x})$. In all tests the background value of $c_{bkg} = 1$. Note that a postprocessing of images was not applied in our numerical tests. All necessary derivatives of the data were calculated using finite differences, just as in all above cited previous publications about numerical studies of the convexification, including two noisy experimental data [26, 27]. Just as in all those works, we have not observed instabilities due to the differentiation, most likely because the step sizes of finite differences were not too small. On Figures 2-7 slices are depicted to demonstrate the values of the computed function $c(\mathbf{x})$.

Test 1. First, we test the reconstruction by our method of a single ball shaped inclusion depicted on Figure 2 a). $c = 2$ inside of this inclusion and $c = 1$ outside. Hence, the inclusion/background contrast is 2:1. We show the 3D image and slices for $N = 1, 3$, see Figures 2.

Test 2. Second, we test the reconstruction by our method of a single elliptically shaped inclusion depicted on Figure 3 a). $c = 2$ inside of this inclusion and $c = 1$ outside. Hence, the inclusion/background contrast is 2:1. We show the 3D image and slices for $N = 1, 3$, see Figures 3.

Test 3. We now test the performance of our method for imaging of two ball shaped inclusions depicted on Figure 4 a). $c = 2$ inside of each inclusion and $c = 1$ outside of these inclusions. Figures 4 display results.

Test 4. We now test our method for the case when the function $c(\mathbf{x})$ is smoothly varying within an abnormality and with a wide range of variations approximately between 0.6 and 1.7. The results are shown in Figure 5. Thus, our method can accurately image not only “sharp” inclusions as in Tests 1-3, but abnormalities with smoothly varying functions $c(\mathbf{x})$ in them as well.

Test 5. In this example, we test the reconstruction by our method of a single ball shaped inclusion with a high inclusion/background contrast, see Figure 6 a). $c = 5$ inside of this inclusion and $c = 1$ outside. Hence, the inclusion/background contrast is 5:1. See Figures 6 for results.

Test 6. In this example we test the stability of our algorithm with respect to the random noise in the data. We test the stability for the case of the function $c(\mathbf{x})$ described in Test 4. The noise is added for $\mathbf{x} \in \Gamma_0$ (see (89)) as:

$$(94) \quad g_{0,\text{noise}}(\mathbf{x}, t) = g_0(\mathbf{x}, t)(1 + \epsilon \xi_t) \text{ and } g_{1,\text{noise}}(\mathbf{x}, t) = g_1(\mathbf{x}, t)(1 + \epsilon \xi_t),$$

where functions $g_0(\mathbf{x}, t), g_1(\mathbf{x}, t)$ are defined in (11), ϵ is the noise level and ξ_t is a random variable depending only on the time t and uniformly distributed on $[-1, 1]$. We took $\epsilon = 5\%$ which is 5% noise.

REFERENCES

- [1] H. AMMARI, J. GARNIER, W. JING, H. KANG, M. LIM, K. SOLNA, AND H. WANG, *Mathematical and Statistical Methods for Multistatic Imaging*, vol. 2098 of Lecture Notes in Mathematics, Springer, Cham, 2013.
- [2] H. AMMARI, Y.T. CHOW, AND J. ZOU, *The concept of heterogeneous scattering and its applications in inverse medium scattering*, SIAM J. Math. Anal., 46 (2014), 2905-2935.
- [3] A. B. BAKUSHINSKII, M. V. KLIBANOV, AND N. A. KOSHEV, *Carleman weight functions for a globally convergent numerical method for ill-posed Cauchy problems for some quasilinear PDEs*, Nonlinear Analysis: Real World Applications, 34 (2017), pp. 201–224.
- [4] L. BAUDOUIN, M. DE BUHAN AND S. ERVEDOZA, *Convergent algorithm based on Carleman estimates for the recovery of a potential in the wave equation*, SIAM J. on Numerical Analysis, 55 (2017), 1578-1613.
- [5] L. BEILINA AND M. V. KLIBANOV, *Approximate global convergence and adaptivity for coefficient inverse problems*, Springer, 2012.
- [6] M. BELLASSOUED AND M. YAMAMOTO, *Carleman Estimates and Applications to Inverse Problems for Hyperbolic Systems*, Springer Japan KK, 2017.
- [7] A. BUKHGEIM AND M. KLIBANOV, *Uniqueness in the large of a class of multidimensional inverse problems*, Soviet Math. Doklady, 17 (1981), pp. 244–247.
- [8] F. CAKONI AND D. COLTON, *Qualitative Methods in Inverse Scattering Theory. An Introduction*, Springer, Berlin, 2006.
- [9] G. CHAVENT, *Nonlinear Least Squares for Inverse Problems - Theoretical Foundations and Step-by-Step Guide for Applications*, Springer, 2009.
- [10] D. COLTON AND R. KRESS, *Inverse Acoustic and Electromagnetic Scattering Theory*, Springer, New York, 3rd ed., 2013.
- [11] A. A. DUCHKOV AND A. L. KARCHEVSKII, *Application of temperature monitoring to estimate the heat flux and thermophysical properties of bottom sediments*, Doklady Earth Sciences, 2014, Vol. 458, Part 2, pp. 1285–1288.
- [12] A.V. GONCHARSKY AND S.Y. ROMANOV, *Iterative methods for solving coefficient inverse problems of wave tomography in models with attenuation*, Inverse Problems, 33 (2017), 025003.
- [13] K. ITO, B. JIN, AND J. ZOU, *A direct sampling method to an inverse medium scattering problem*, Inverse Problems 28 (2012), 025003.
- [14] K. ITO, B. JIN, AND J. ZOU, *A direct sampling method for inverse electromagnetic medium scattering*, Inverse Problems 29 (2013), 095018.
- [15] S. I. KABANIKHIN, A. D. SATYBAEV, AND M.A. SHISHLENIN, *Direct Methods of Solving Multidimensional Inverse Hyperbolic Problem*, VSP, Utrecht, 2004.

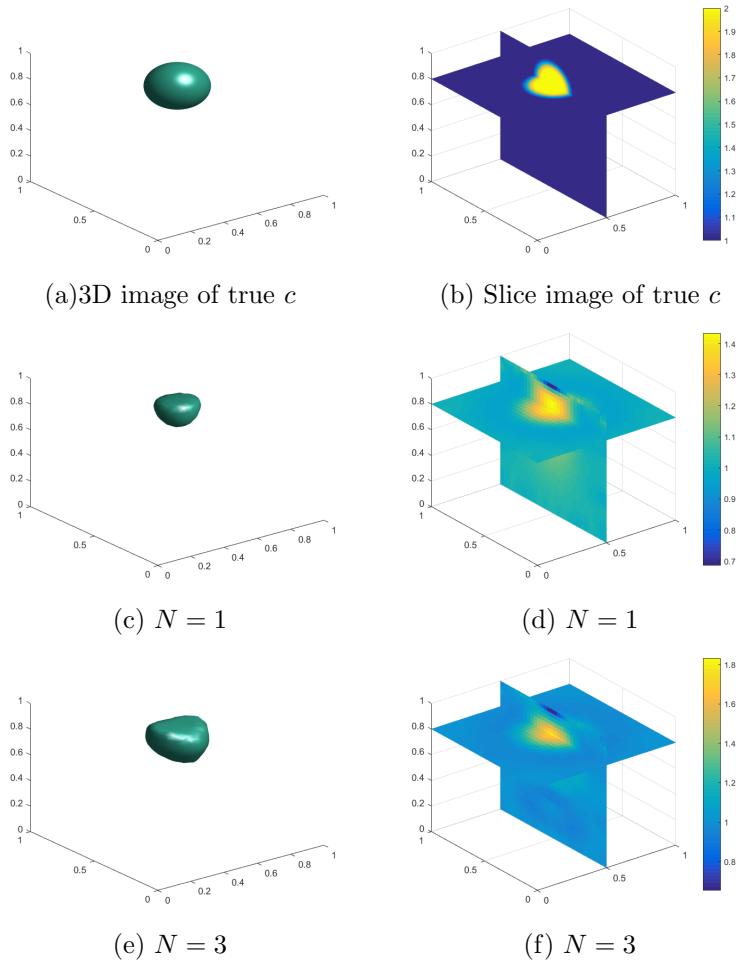


FIG. 2. Results of Test 1. Imaging of one ball shaped inclusion with $c = 2$ in it and $c = 1$ outside. Hence, the inclusion/background contrast is 2:1. We have stopped at the 3rd mesh refinement for all three values of N . a) and b) Correct images. c) and d) Computed images for $N = 1$. e) and f) Computed images for $N = 3$. The maximal value of the computed coefficient $c(\mathbf{x})$ is approximately 1.8.

- [16] S.I. KABANIKHIN, K.K. SABELFELD, N.S. NOVIKOV, AND M.A. SHISHLENIN, *Numerical solution of the multidimensional Gelfand-Levitan equation*, J. Inverse and Ill-Posed Problems 23 (2015), pp. 439-450.
- [17] M.V. KLIBANOV AND O.V. IOUSSOUPOVA, Uniform strict convexity of a cost functional for three-dimensional inverse scattering problem, SIAM J. Math. Anal., 26 (1995), pp. 147-179.
- [18] M.V. KLIBANOV, *Global convexity in a three-dimensional inverse acoustic problem*, SIAM J. Math. Anal., 28 (1997), pp. 1371-1388.
- [19] M.V. KLIBANOV, *Global convexity in diffusion tomography*, Nonlinear World, 4 (1997), pp. 247-265.
- [20] M. V. KLIBANOV AND A. TIMONOV, *Carleman Estimates for Coefficient Inverse Problems and Numerical Applications*, de Gruyter, Utrecht, 2004.
- [21] M. V. KLIBANOV, *Carleman estimates for global uniqueness, stability and numerical methods for coefficient inverse problems*, J. Inverse and Ill-Posed Problems, 21 (2013), pp. 477-560.
- [22] M. V. KLIBANOV, *Carleman weight functions for solving ill-posed Cauchy problems for quasi-linear PDEs*, Inverse Problems, 31 (2015), 125007.
- [23] M. V. KLIBANOV AND N. T. THÀNH, *Recovering dielectric constants of explosives via a globally*

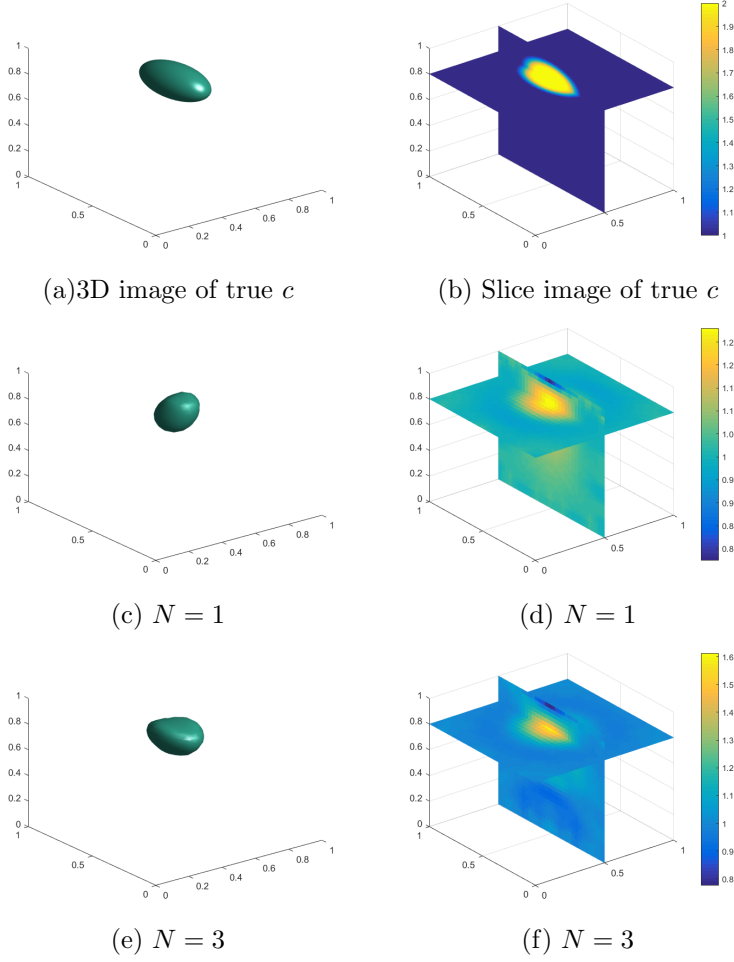


FIG. 3. Results of Test 2. Imaging of one elliptically shaped inclusion with $c = 2$ in it and $c = 1$ outside. Hence, the inclusion/background contrast is 2:1. We have stopped at the 3rd mesh refinement for all three values of N . a) and b) Correct images. c) and d) Computed images for $N = 1$. e) and f) Computed images for $N = 3$. The maximal value of the computed coefficient $c(\mathbf{x})$ is approximately 1.6.

- strictly convex cost functional*, SIAM J. Appl. Math., 75 (2015), pp. 518–537.
- [24] M. V. KLIBANOV, A. E. KOLESOV, L. NGUYEN, AND A. SULLIVAN, *Globally strictly convex cost functional for a 1-D inverse medium scattering problem with experimental data*, SIAM J. Appl. Math., 77 (2017), pp. 1733–1755.
 - [25] M. V. KLIBANOV AND A. E. KOLESOV, *Convexification of a 3-D coefficient inverse scattering problem*, Computers and Mathematics with Applications, published online, <https://doi.org/10.1016/j.camwa.2018.03.016>, 2018.
 - [26] M. V. KLIBANOV, A. E. KOLESOV, L. NGUYEN, AND A. SULLIVAN, *A new version of the convexification method for a 1D coefficient inverse problem with experimental data*, Inverse Problems, 34 (2018), 115014.
 - [27] M. V. KLIBANOV, A. E. KOLESOV, D.-L. NGUYEN, *Convexification method for an inverse scattering problem and its performance for experimental backscatter data for buried targets*, arXiv: 1805.07618, 2018.
 - [28] M.V. KLIBANOV, J. LI, AND W. ZHANG, *Electrical impedance tomography with restricted Dirichlet-to-Neumann map data*, arXiv:1803.11193, 2018.
 - [29] A. LAKHAL, *A decoupling-based imaging method for inverse medium scattering for Maxwell's*

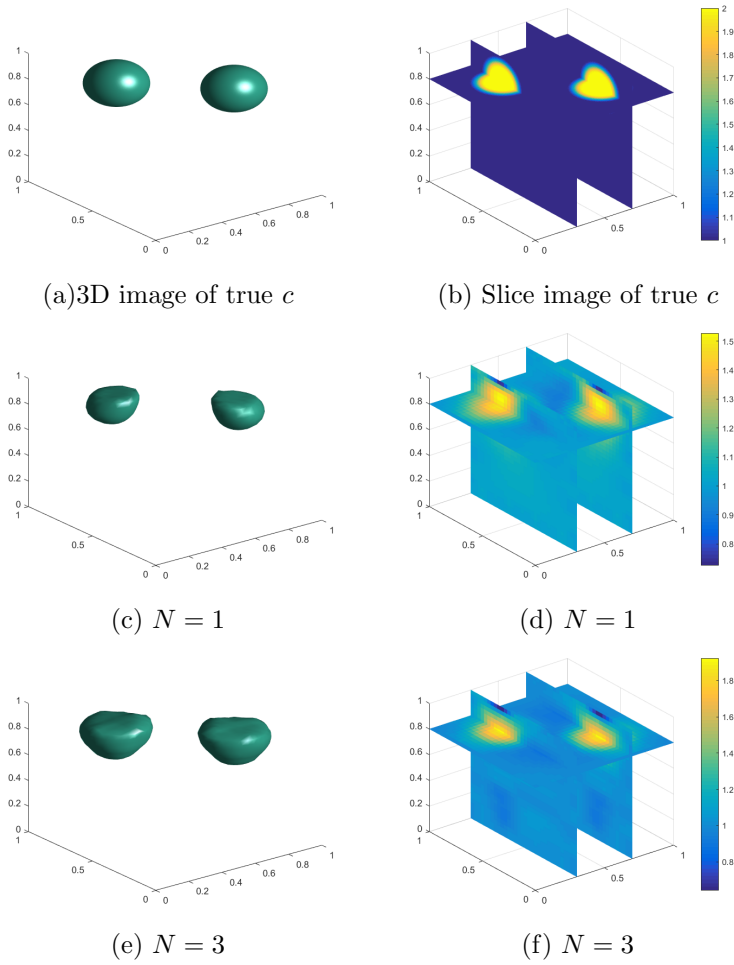


FIG. 4. Results of Test 3. Imaging of two ball shaped inclusions with $c = 2$ in each of them and $c = 1$ outside. We have stopped on the 3rd mesh refinement for all three values of N . a) and b) Correct images. c) and d) Computed images for $N = 1$. e) and f) Computed images for $N = 3$. In each imaged inclusion, the maximal value of the computed coefficient $c(\mathbf{x})$ is approximately 1.9.

equations, Inverse Problems, 26 (2010), 015007.

- [30] J. LI AND J. ZOU, *A multilevel model correction method for parameter identification*, Inverse Problems 23 (2007), 1759.
- [31] J. LI, H. LIU, AND Q. WANG, *Enhanced multilevel linear sampling methods for inverse scattering problems*, J. Comput. Phys., 257 (2014), pp. 554–571.
- [32] J. LI, P. LI, H. LIU, AND X. LIU, *Recovering multiscale buried anomalies in a two-layered medium*, Inverse Problems, 31 (2015), 105006.
- [33] G. RIZZUTI AND A. GISOLF, *An iterative method for 2D inverse scattering problems by alternating reconstruction of medium properties and wavefields: theory and application to the inversion of elastic waveforms*, Inverse Problems 33 (2017), 035003.
- [34] V.G. ROMANOV, *Inverse Problems of Mathematical Physics*, VNU Press, Utrecht, 1986.
- [35] V.G. ROMANOV, *Inverse problems for differential equations with memory*, Eur. J. Math. Comput. Appl., 2 (2014), pp. 51–80.
- [36] A.N. TIKHONOV, A.V. GONCHARSKY, V.V. STEPANOV AND A.G. YAGOLA, *Numerical Methods for the Solution of Ill-Posed Problems*, Kluwer, London, 1995.
- [37] M.M. VAJNBURG, *Variational Method and Method of Monotone Operators in the Theory of Nonlinear Equations*, John Wiley& Sons, Washington, DC, 1973.

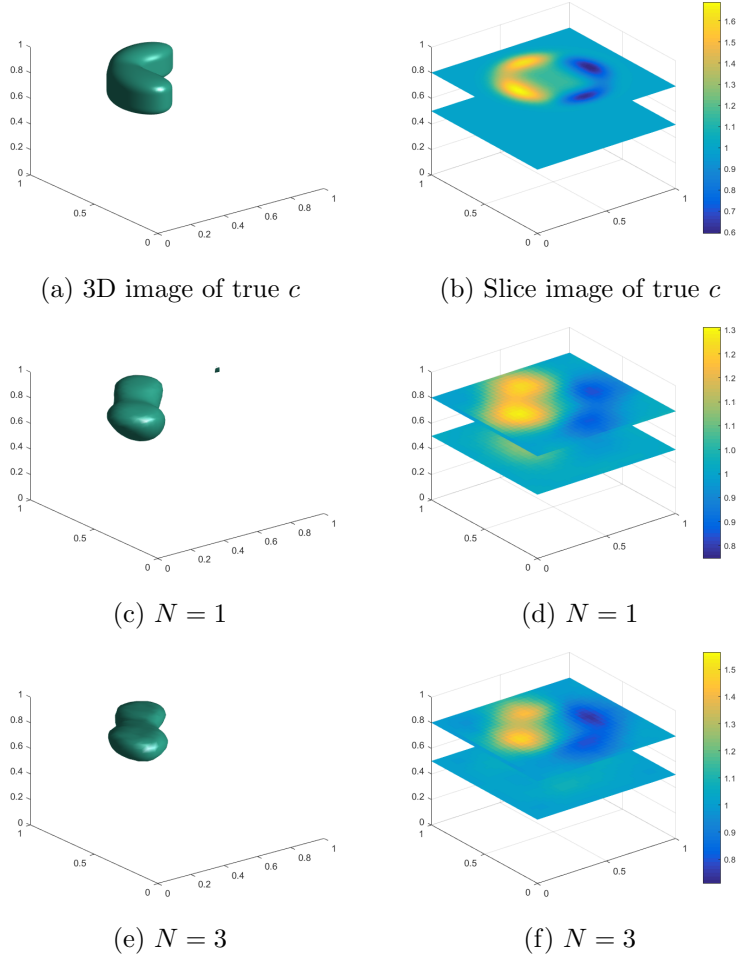


FIG. 5. Results of Test 4. Imaging of a smoothly varying coefficient. The function $c(\mathbf{x})$ in the inclusion varies between 0.4 and 1.6. a) and b) Correct images. c) and d) Computed images for $N = 1$. e) and f) Computed images for $N = 3$. The computed function $c(\mathbf{x})$ in the inclusion varies approximately between 0.7 and 1.6.

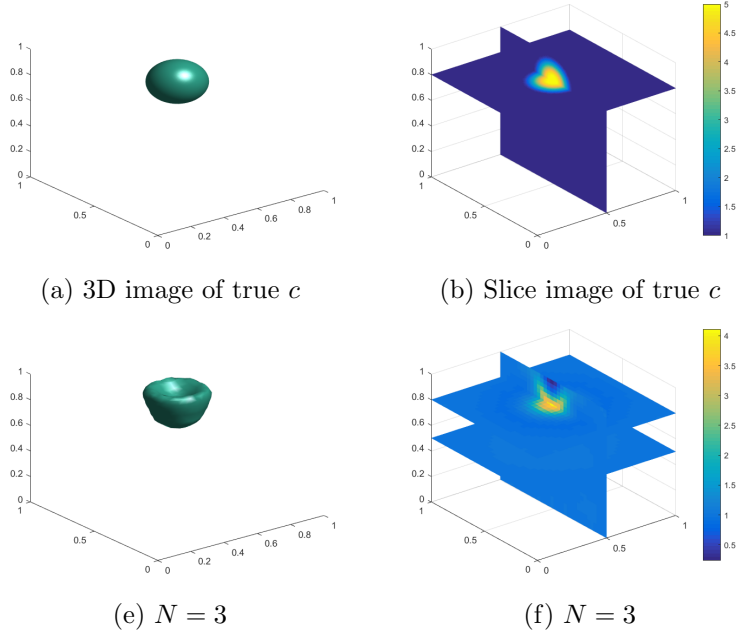


FIG. 6. Results of Test 5. Imaging of one ball shaped inclusion with $c = 5$ in it and $c = 1$ outside. Hence, the inclusion/background contrast is 5:1. We have stopped at the 3rd mesh refinement. a) and b) Correct images. c) and d) Computed images for $N = 3$. The maximal value of the computed coefficient $c(\mathbf{x})$ is approximately 4.

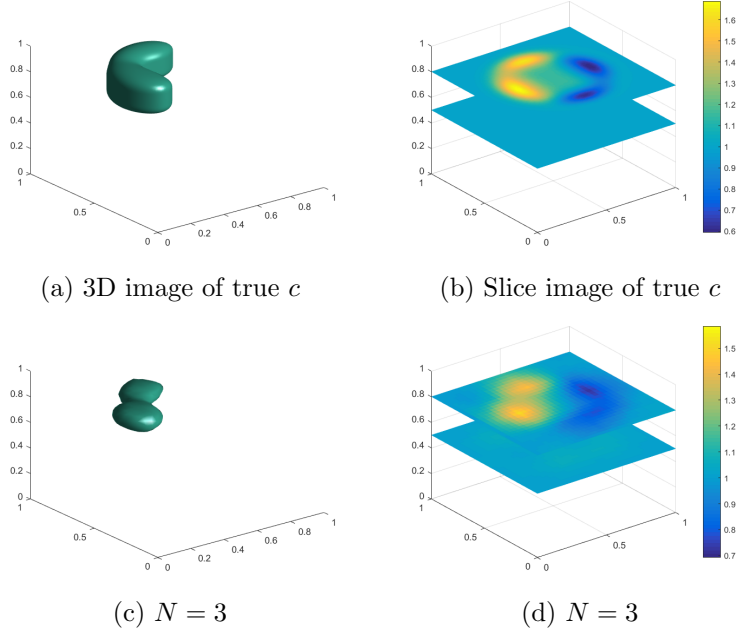


FIG. 7. Results of Test 6. We test the reconstruction of the same function $c(\mathbf{x})$ as in Test 4 (Figures 5) but with the noise in the data. The level of noise in (94) is $\epsilon = 5\%$. We have stopped at the 3rd mesh refinement for $N = 3$. a) and b) Correct images. c) and d) Computed images for $N = 3$. The computed function $c(\mathbf{x})$ in the inclusion varies between 0.7 and 1.6.